

Effect of Biomineralized Manganese on the Corrosion Behavior of C1008 Mild Steel

B.H. Olesen, P.H. Nielsen, and Z. Lewandowski*

ABSTRACT

The possibility that biomineralized manganese dioxide (MnO_2) might serve as an efficient cathodic reactant in mild steel corrosion was studied using stainless steel (SS) covered with microbially or electrochemically deposited MnO_2 and galvanically coupled to mild steel and mild steel covered with microbially deposited MnO_2 . Biofilms of the manganese-oxidizing bacteria, *Leptothrix discophora* SP-6, were used to deposit biomineralized MnO_2 . When MnO_2 was biologically deposited on the SS, the corrosion rate of the galvanically coupled mild steel was initially about eight times higher than that in a control experiment without depositing manganese. After a few minutes, the MnO_2 discharged and the corrosion rate of the mild steel decreased to values comparable with biofouled cathodes without manganese. When MnO_2 was electroplated on SS, a linear relation between the amount of MnO_2 and the duration of the elevated corrosion rate of mild steel was observed. However, when MnO_2 was biologically deposited directly onto the mild steel, the corrosion rate did not increase, possibly because the corrosion product buildup on the mild steel surface prevented electrical contact between the manganese oxide and the underlying metal.

KEY WORDS: biomineralization, electrochemical impedance spectroscopy, galvanic corrosion, *Leptothrix discophora* SP-6, manganese dioxide, microbiologically influenced corrosion, mild steel, UNS G10080

INTRODUCTION

The influence of biomineralization on corrosion processes has become an important new subject of study for corrosion engineers and microbiologists. Particularly, manganese biomineralization and the deposition of cathodically active manganese dioxide (MnO_2) have received much attention.¹⁻¹⁰ Recent studies at the Center for Biofilm Engineering showed that microbially deposited MnO_2 on type 316L (UNS S31603)⁽¹⁾ stainless steel (SS) samples in a fresh water stream shifted the corrosion potential from -150 mV_{SCE} to $\sim 400 \text{ mV}_{SCE}$.^{1,2} It was discovered that the potential of such ennobled steel samples positively correlated with the amount of deposited manganese mineral and with the number of manganese-oxidizing bacteria on the surface.³ Similar effects were obtained by covering the steel with a hydrous MnO_2 paste.² The ennoblement of microbially colonized passive metals is well known and numerous theoretical explanations for this phenomenon have been given.^{7,11} Recent studies have shown a correlation between the amount of biomineralized manganese deposited and the extent of ennoblement, which induced questions regarding the role of manganese in microbially influenced corrosion.

The results correspond well with the inspection of severely corroded SS turbine runner blades in a Dutch hydroelectric power plant, where large amounts of manganese minerals, mainly manganese oxyhydroxide ($MnOOH$) and MnO_2 , were found on the steel surface.^{4,5} Since the steel types used to make the runner blades were resistant to pitting corrosion

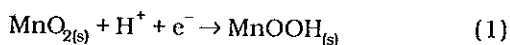
Submitted for publication October 1998; in revised form, September 1999.

* Center for Biofilm Engineering, EPS 366, Montana State University, Bozeman, MT 59717-3980.

⁽¹⁾ UNS numbers are listed in *Metals and Alloys in the Unified Numbering System*, published by the Society of Automotive Engineers (SAE) and cosponsored by ASTM.

at the reported chloride concentration, the investigators suggested that the pitting corrosion was caused by the presence of manganese minerals on the surface. An investigation of galvanic corrosion in a marine environment showed increased corrosion rates if the cathodes were ennobled through fouling by marine biofilms.⁹ A German company investigating pitting corrosion in a cooling water distribution system reported similar observations.¹² The type 316 Ti SS pipes used to pump cooling water from the river Rhine were pitted severely around welds, which was associated hypothetically with the presence of iron- and manganese-oxidizing bacteria.⁹

Biominedralized MnO₂ deposited on electrically conducting surfaces can provide a powerful cathodic reaction, of which the extent is limited only by the amount of biologically deposited material and the nature of the anodic reaction. The electrochemical reduction of MnO₂ on a SS surface, at neutral pH, proceeds over MnOOH to divalent manganese (Mn²⁺) through:⁷⁻⁸



However, to understand the possible influence of MnO₂ on corrosion, it is important to consider the cathodic and anodic reactions. Consequently, the existence of a manganese redox cycle on metal surfaces was hypothesized, where the manganese-oxidizing bacteria deposit the minerals and the cathodic electrochemical reduction dissolves the minerals. The supply of electrons would come from a corroding anodic site on the same metal surface. Such a scenario would be dangerous primarily for mild steels because of high corrosion currents and resulting high turnover rate of the manganese cycle. In this study, how the galvanic couple of SS and mild steel behaves when the SS is covered with MnO₂, and how mild steel behave when exposed to cultures of manganese-depositing bacteria was studied. Can the biominedralized MnO₂ increase the corrosion rate of mild steel?

EXPERIMENTAL PROCEDURES

The following experiments were designed to provide answers to the above question. Experiments 1(a) and (b) were significantly different from Experiment 2 in that they involved separate SS cathodes and mild steel anodes. Experiment 2 involved only mild steel samples, where cathodes and anodes coexisted on the same mild steel surface.

Experiment 1(a)

To find out if the cathodic reduction of biominedralized MnO₂ increases the anodic dissolution rate of mild steel, a C1008 mild steel anode was galvanically coupled to a SS cathode, so the cathode and anode were separated. Prior to connecting the two electrodes, MnO₂ was biologically deposited on the SS cathode using biofilms of manganese-oxidizing bacteria, *Leptothrix discophora* SP-6. Similar galvanic couples with clean cathodes were used as controls. The galvanic setup enabled direct measurements of the corrosion current, which was used to calculate the corrosion rate of the mild steel.

Experiment 1(b)

To measure the rates of these reactions, galvanic couples were assembled using cathodes electroplated with known amounts of MnO₂. The current generated as a result of MnO₂ reduction was maintained subsequently.

Experiment 2

To monitor the direct effect of MnO₂ on mild steel corrosion rate, mild steel samples were covered with MnO₂ depositing biofilms of *L. discophora*. This setup prevented direct measurements of the corrosion current between the anode and cathode. Consequently, corrosion rates were measured using electrochemical impedance spectroscopy (EIS), a technique that does not affect bacterial growth and activity significantly.¹³

Corrosion Coupons

Mild steel (C1008 [UNS G10080]) and SS (type 316L) coupons, 16.8 mm (2/3 in.) in diameter, were punched out of 1.6-mm (16-gauge) cold-rolled sheet metal. Compositions of the two steel types used are shown in Tables 1 and 2.

Coupons were sonicated in acetone (CH₃COCH₃), in distilled water, air dried, and epoxy was embedded in cylindrical polycarbonate holders using a slow-hardening epoxy (Buehler Epoxide¹). The metal surfaces were polished on a series of sandpaper ranging from 120 grit to 600 grit. A steel spring soldered to a copper wire and pressed against the back of the coupon through a rubber stopper served as electrical connection. The resistance of each connection was measured, and only the coupons showing an electrical resistance < 1 Ω were accepted. Coupons with holders and connectors were sterilized by soaking in 95% ethanol (C₂H₅OH) for 5 min followed by exposure to ultraviolet (UV) light in a laminar flow hood for 12 h.

Inoculum and Growth Medium

Manganese-oxidizing bacteria *Leptothrix discophora* SP-6 were obtained (freeze-dried) from American Type Culture Collection¹ (ATCC no. 51168).¹⁴ The organisms were grown in a mineral-

¹ Trade name.

TABLE 1
Elemental Composition of C1008 Mild Steel (wt%)

Fe	Mn	C	Al	F	Si	S
Bal.	0.244	0.05	0.031	0.015	0.014	0.013

salt-pyruvate-vitamin (MSPV) medium (ATCC no. 1917). Filter-sterilized solutions of vitamins, pyruvate, and in some cases, manganese sulfate ($MnSO_4$) was added aseptically after autoclaving for 15 min/L at 121°C and 2 atm. Subcultures were concentrated by centrifugation, resuspended in MSPV medium containing 10% glycerol, and preserved by freezing at -70°C.¹⁵ Reactors were inoculated using 10 mL of a thawed culture incubated for 48 h in 100 mL MSPV medium. The original MSPV media was modified for use in continuously fed reactors. The concentrations of carbon source (pyruvate), nitrogen source (ammonium sulfate), and vitamins were reduced to 25% and the buffer (HEPES¹) was reduced to 10% relative to the original recipe. Five times the concentrated medium was used and it was mixed with dilution water just before pumping it into the reactors.

Reactors

The setup for biological deposition of MnO_2 consisted of ≈ 700 mL, cylindrical polycarbonate reactors with removable tops and bottoms (Figure 1). Each top had eight holes for insertion of eight coupon holders plus holes for media input and output, air input and output, and a saltbridge. A graphite disc counter electrode was fixed to the bottom of each reactor. Electrical connection between the reactor and a saturated calomel reference electrode (SCE) was made through salt bridges containing 1% agar and 1 mM sodium sulfate (Na_2SO_4).³ The reactor end of the salt bridge was sealed by a porous glass plug. This allowed the bridge to be filled after the reactors were autoclaved and to avoid formation of air bubbles within the agar. The salt bridge was placed in the center of the reactor, and after autoclaving the reactors for 20 min at 121°C and 2 atm, eight corrosion coupons were placed peripheral 35 mm (1-3/8 in.) from the bridge. The crevice between the coupon holder and reactor lid was sealed with an O-ring. Figure 2 shows the flowchart of media: dilution water and air to and from the reactor. Filtered (0.2 μ) atmospheric air was pumped at a rate of ≈ 300 cm³/min (18 in.³/min) into the reactor through a porous stone. The stone was placed at a level between the tip

of the salt bridge and the surface of the media to avoid accumulation of air bubbles at the corrosion coupons. Air outlet from the headspace also was filtered to avoid back contamination. Sterilized growth medium (one part concentrated autoclaved medium and four parts filtered dilution water) was supplied to the bottom of the reactor at a rate of 500 mL/day. Deionized water was filtered first through a 10- μ m filter, then through a 0.2- μ m filter (both Whatman, Polycap AS¹) and used as dilution water. Effluent was pumped out from the top of the reactor at a higher rate. The liquid volume in the reactor was adjusted to 500 mL by positioning the effluent tube.

SS Cathode Covered with Biomineralized MnO_2 —

For the galvanic experiment with biologically deposited MnO_2 , two separate reactors (1A-1 and 1A-2), each with eight sterilized SS coupons, were prepared as described. $MnSO_4$ was added to the media supply for one reactor (1A-2), so that the final concentration of manganese in the reactor was 100 μ M. Both reactors were inoculated with *L. discophora* as described. After 48 h of running the reactors in a batch mode, allowing attachment of bacterial cells, the reactors were run in a continuous mode for 2 weeks. Open-circuit potential (OCP) of all coupons were recorded daily versus the SCE reference electrode using a hand-held multimeter (internal resistance: 10 m). Subsequently, the ennobled SS samples were removed from the reactor and immersed with a clean mild steel coupon in a dual cell containing a 0.1-M Na_2SO_4 solution of pH 6.5.¹⁶ The dual cell setup consisted of two beakers connected through a salt bridge, sealed with porous glass, containing the same electrolyte. This way, iron minerals/ions from the anodic reactions at the mild steel surface were prevented from interfering with the cathodic reactions on the SS surface. The two coupons (one ennobled SS cathode and one clean mild steel anode) were placed separately, one in each of the two beakers and short-circuited through a zero-resistance ammeter (EG&G Princeton Applied Research¹, potentiostat/galvanostat model 273A). The current that flowed between the two coupons was measured every second for 1 h. The initial corrosion rate, (average of the first 100 s) and the final corrosion rate (after 30 min) were calculated based on the current measurements: the density (7.85 g/cm³ [128.6 g/in.³]) of the mild steel and the equivalent weight (27.92 g/eq) of iron.

SS Cathode Electroplated with MnO_2 — MnO_2 was galvanostatically plated onto SS coupons in 0.1 M

TABLE 2
Elemental Composition of Type 316L Stainless Steel (wt%)

Fe	Cr	Ni	Mo	Mn	Si	Cu	Co	P	C	S
Bal.	16.60	10.17	2.08	1.78	0.36	0.25	0.12	0.030	0.019	0.014

Na_2SO_4 containing 5 mM MnSO_4 at pH 6.5 and room temperature. Increasing amounts of charge (100 mC/cm², 200 mC/cm², 300 mC/cm², and 400 mC/cm² [15.5 mC/in.², 31 mC/in.², 46.5 mC/in.², and 62 mC/in.²]) were transferred at 0.1 mA/cm² (15.5 A/in.²) for different steel samples corresponding to various amounts of deposited oxide. A charge of 100 mC corresponded to 45 μg MnO_2 . The composition of the plated mineral was analyzed by x-ray photoelectron spectroscopy (XPS), as described elsewhere,⁷ and found to match a commercial MnO_2 standard (99% pure). Subsequently, each plated SS coupon was immersed along with a mild steel coupon in the dual cell containing 0.1 M Na_2SO_4 at pH 6.5. The two coupons were short-circuited and the current was measured as described in the previous experiment. A reference experiment in which the SS had not been electroplated was performed in the same way.

Mild Steel Covered with Biomineralized MnO_2 —

The experimental setup for uniform corrosion of mild steel consisted of three reactors (2-1, 2-2, and 2-3), prepared as described, each with eight sterilized coupons (five C1008 mild steel and three type 316L SS) mounted. The SS coupons were used to identify ennoblement and thus manganese biomineralization. MnSO_4 was added to the media for two of the three reactors (2-1 and 2-2), so that the final concentrations of manganese in the reactors were 100 μM . The third reactor (2-3) was operated without manganese. One of the reactors with manganese (2-2) and the reactor without manganese (2-3) were inoculated with *L. discophora*. Consequently, the experimental setup included one reactor without bacteria but with manganese (2-1), one reactor with bacteria and manganese (2-2), and one with bacteria but no manganese (2-3). The setup enabled the separation of the effect of biofilms and manganese on the corrosion rate of mild steel to pursue the effect of biomineralized manganese alone. Reactors were run for 48 h in batch mode, allowing attachment of the microorganisms, whereupon the reactors were switched to a continuous mode for 2 weeks, until all measured parameters reached steady state. OCP of the SS samples were recorded daily.

Corrosion rates of the C1008 mild steel samples were determined by electrochemical impedance spectroscopy (EIS). The method is used frequently in microbially influenced corrosion (MIC)¹⁷ and was chosen because of its negligible effect on bacterial activity.¹³ The analysis was performed using a potentiostat/galvanostat (EG&G Princeton Applied Research,¹ model 273A) and a frequency response analyzer (Solartron Slumberger,¹ model SI1255). Two parallel-coupled multiplexers (Scribner Associates, Inc.,¹ model 314) allowed for 15 inputs to the potentiostat. All reference electrode inputs to the multiplexers were connected to a single SCE that,

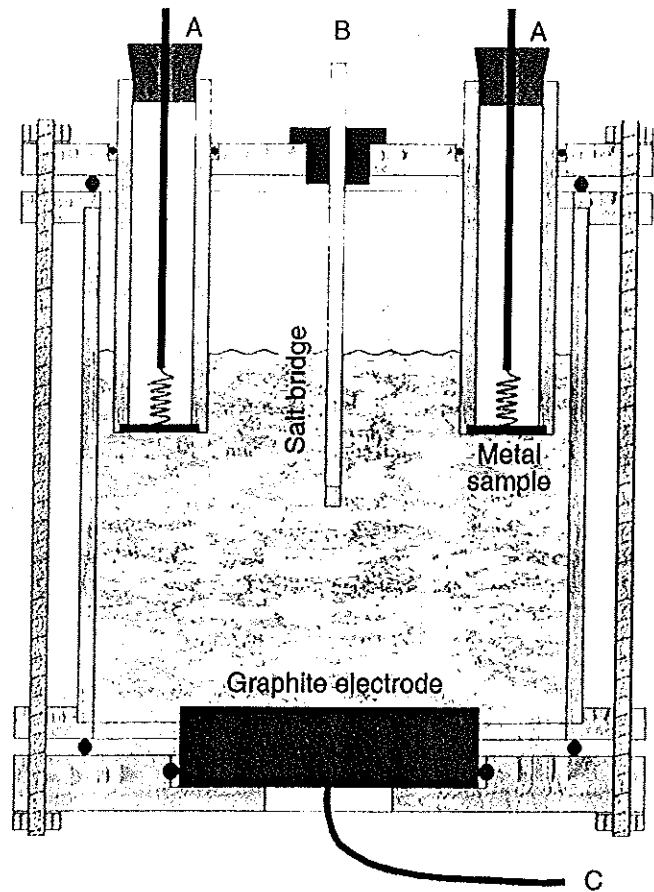


FIGURE 1. Experimental reactor used for biofilm growth with connections to: (A) a working electrode, (B) a reference electrode through a SCE, and (C) a counter electrode.

through tubing filled with 0.1 M Na_2SO_4 , was connected to the salt bridges in the three reactors. Five counter electrode inputs (one for each mild steel coupon) were connected to the carbon disk counter electrode in each of the three reactors. The working electrode inputs were connected to each of the mild steel corrosion coupons. To control the experiment and collect data, a commercially available software, Zplot[†] (Scribner Associates, Inc., version 2.0 for Windows), was used.

An alternating current (AC) signal with a 10-mV amplitude and frequencies ranging from 100,000 Hz to 0.01 Hz was applied to the sample at OCP. The resulting current was measured and used to calculate impedance and phase angle. The impedance also was divided into a real (Z') and an imaginary (Z'') part, that when plotted against each other, created two semicircles on the real axis.

The validity of the experimental impedance data was tested using the Kramers-Kronig Transforms,¹⁸ which converts the real part of the impedance into the imaginary part and vice-versa. If the original data set fulfilled causality, linearity, and stability, and if the transferred function had finite boundary values

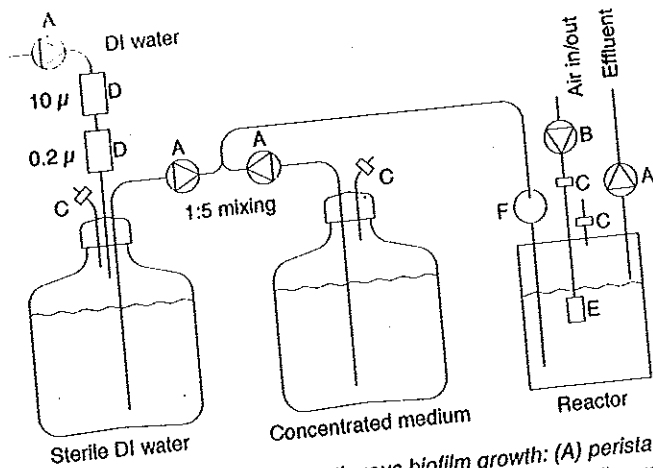


FIGURE 2 Setup used for continuous biofilm growth: (A) peristaltic pump, (B) air pump, (C) bacterial air vent, (D) water filter, (E) porous stone, (F) air lock. (500 mL media in reactor; 500 mL/h fresh feed). DI represents deionized water.

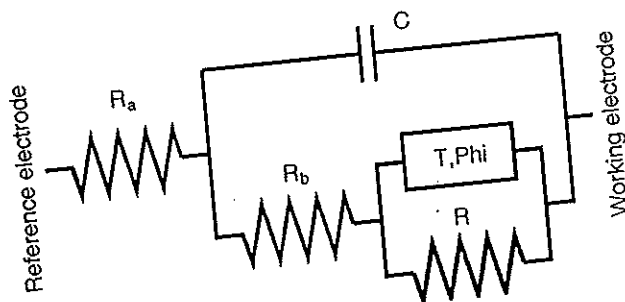


FIGURE 3. Equivalent circuit model used to fit electrochemical impedance data.

at $\omega \rightarrow 0$ and $\omega \rightarrow \infty$, then the original and calculated impedance data should have overlapped each other.¹⁸⁻¹⁹ Except for a few rejected cases, this condition was fulfilled for all collected data.

In the complex plane representation of Z' and Z'' , the two semicircles represents the electrolyte resistance (the circle closest to origin, usually the smallest) and the polarization resistance, respectively. Fitting a circle to the right-most semicircle of the experimental data and subtracting the low intercept with the real axis from the high intercept yielded a good approximation to the polarization resistance. An approximate value for the double-layer capacitance was obtained from the frequency (ω_{max}) at the maximum of the right-most semicircle through:²⁰

$$C = \frac{1}{R\omega_{max}} \quad (3)$$

Using these approximate values for resistance (R) and capacitance (C), the impedance data was fitted

with an equivalent circuit model that included a distributed Zarc-Cole element to account for diffusion-controlled reactions (illustrated by semicircles depressed into the fourth quadrant, Figure 3).²¹⁻²² The impedance of the Zarc-Cole element is determined by:

$$Z = \frac{R_z}{1 + R_z T (i\omega)^{Phi}} \quad (4)$$

where Phi determines the depression. For Phi = 1, the center of the semicircle lies on the real axis, and as Phi approaches 0, the center of the circle is depressed into the fourth quadrant. In the shown equivalent circuit, R_a represents the electrolyte resistance from the working electrode to the reference, C represents the capacitance of the double layer, and R_b and R_z represent the polarization resistance. The inverse sum of R_b and R_z served as a relative representation of the corrosion rate:²³

$$I_{corr} = \frac{\beta_a \beta_c}{2.303(\beta_a + \beta_c)} \frac{1}{R_p} \approx \frac{B}{R_p} \quad (5)$$

RESULTS

SS Cathode Covered with Biomineralized MnO₂ — MnO₂ was microbially deposited on the SS cathodes in the reactor with Mn²⁺ (1a-2). OCP of the coupons stabilized at 390 mV_{SCE} ± 5 mV_{SCE} within 3 days of exposure, whereas the potential of the samples in the control reactor without manganese (1a-1) remained unchanged at -100 mV_{SCE} ± 20 mV_{SCE}. Three days after inoculation, the biofilm in both reactors was visible (brownish in the reactor with manganese as a result of mineral deposition) and grew thicker and less patchy as the experiment progressed. Coupling the biofouled SS cathodes to the mild steel anodes after 2 weeks of biofilm growth showed that the galvanic current, and thus, the corrosion rate, was between 4 and 11 times higher than time control for cathodes from the reactor with manganese compared to the control reactor without manganese (Figure 4). Without manganese, the current was between 10 mA/cm² and 50 mA/cm² (1.5 mA/in.² and 7.75 mA/in.²), whereas with manganese it was 150 mA/cm² to 210 mA/cm² (23.25 mA/in.² to 32.5 mA/in.²). The elevated current lasted only for ~ 3 min to 5 min, after which time it returned to values similar to the control samples without manganese.

SS Cathode Electroplated with MnO₂ — When the SS cathodes were electroplated with MnO₂ before coupling to mild steel anodes, the galvanic current between the two samples was increased initially in way similar to that in the microbial experiments.

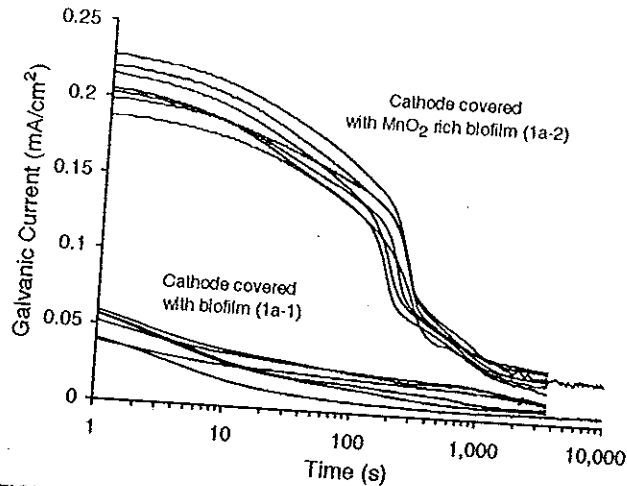


FIGURE 4. Current drawn from the galvanic couple of C1008 mild steel and type 316L SS with MnO_2 biologically plated on the SS cathode (1a-2). SS cathode with mineral-free *L. discophora* biofilm used as reference (1a-1).

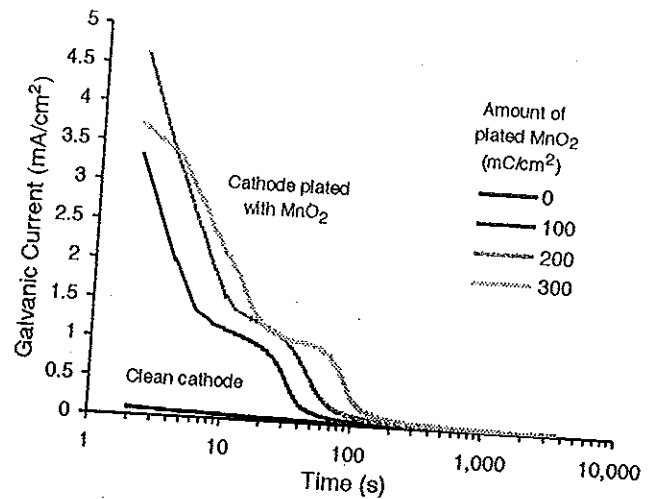


FIGURE 5. Current drawn from the galvanic couple of C1008 mild steel and type 316L SS with MnO_2 electroplated on the SS cathode. SS cathode without plated mineral used as reference.

With manganese, the initial current was 1 mA/cm² to 5 mA/cm² (155.5 μ A/in.² to 775 μ A/in.²). In the control experiment, without manganese, only 0.1 mA/cm² (15.5 μ A/in.²) was drawn between the two samples. OCP of the plated cathodes were stable at 520 mV_{SCE} \pm 30 mV_{SCE}. Figure 5 shows changes in the galvanic current for samples with different amounts of deposited oxide. For galvanic couples with manganese, the current returned to values similar to the control experiment after 2 min to 5 min of short-circuiting. The magnitude and duration of the elevated current depended directly upon the amount of manganese mineral present on the cathode. Consequently, the initial corrosion rate and the total amount of iron dissolved increased as a function of the amount of MnO_2 deposited on the surface (Table 3).

Mild Steel Covered with Biomineralized MnO_2 — Experiments did not reveal significantly different corrosion rates in the reactors (Figure 6): (2-1) with manganese and without *L. discophora*, (2-2) with manganese and *L. discophora*, and (2-3) with *L. discophora* and without manganese. Steady OCP for

the SS samples in all three reactors were reached after 3 to 4 days of the experiment (Figure 7). SS coupons in Reactor 2-2 showed a typical MnO_2 -induced ennoblement with OCP of 300 mV_{SCE} \pm 6 mV_{SCE},^{2-3,7-8} whereas samples in Reactors 2-1 and 2-3 stabilized at 68 mV_{SCE} \pm 10 mV_{SCE} and 88 mV_{SCE} \pm 11 mV_{SCE}, respectively.

Impedance data collected from the mild steel samples satisfied, with a few exceptions, the Kramers-Kronig transformations.¹⁸ The collected spectra were fitted with the circuit shown in Figure 3 to obtain values for $R_z + R_b$, R_a , and surface C. During the first 3 days, the extracted values were unstable for all analyzed spectra. Consequently, data for the first 3 days were not included.

The R_a remained constant, \sim 110 Ω to 140 Ω , during the experiment. There was a slight difference between the solution resistance in the reactors (2-1 and 2-2) with manganese and the reactor (2-3) without manganese. The surface C stabilized at 223 nF \pm 6 nF, 175 nF \pm 3 nF, and 204 nF \pm 12 nF for Reactors 2-1, 2-2, and 2-3, respectively. $R_z + R_b$ reached stable values of 1,380 Ω \pm 75 Ω , 1,200 Ω \pm

TABLE 3
Initial^(A) and Final^(B) Corrosion Rate and the Total Amount of Dissolved Iron
From the Galvanic Couple of C1008 Mild Steel and MnO_2 -Plated Stainless Steel

Amount of MnO_2		Initial Corrosion Rate [MMPY]	Final Corrosion Rate [MMPY]	Total Dissolved Iron	
[mC/cm ²]	[mC/in. ²]			[μ g/cm ²]	[μ g/in. ²]
0	0				
100	15.5	0.5	0.19	8.9	1.38
200	31	11.8	0.21	23.6	3.66
300	46.5	16.3	0.20	35.2	5.46
		18.8	0.17	49.9	7.73

^(A) Average of the first 100 s.

^(B) After 30 min.

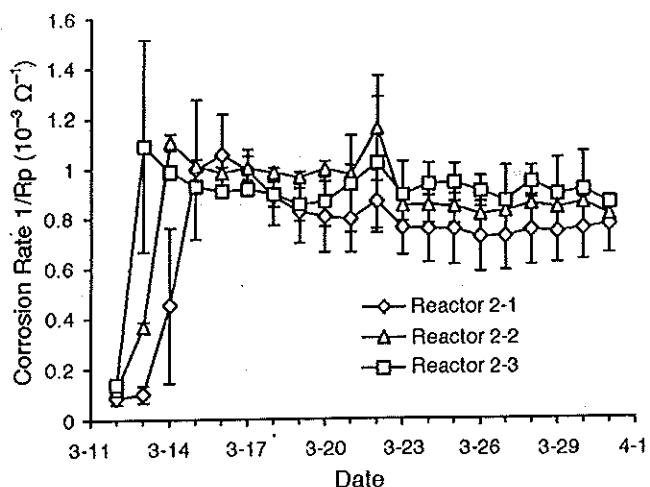
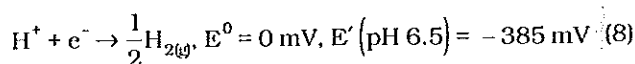
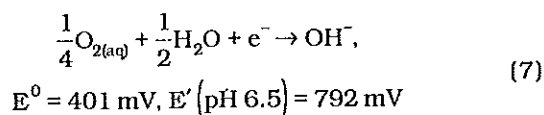
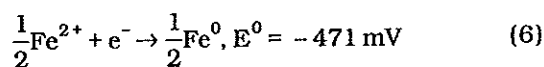


FIGURE 6. Corrosion rate of mild steel illustrated as the inverse polarization resistance. 2-1: growth media with manganese, 2-2: growth media with manganese and bacteria, 2-3: growth media with bacteria.

30 Ω , and $1,130 \Omega \pm 55 \Omega$ for Reactors 2-1, 2-2, and 2-3, respectively. The corrosion rate, calculated as the inverse of the polarization resistance (Figure 6), leveled out at $750 \pm 40 \times 10^{-6} \Omega^{-1}$, $840 \pm 20 \times 10^{-6} \Omega^{-1}$, and $905 \pm 35 \times 10^{-6} \Omega^{-1}$, respectively.

DISCUSSION

The processes involved in metallic corrosion usually are presented in a simplified form composed of the anodic dissolution of the base metal, in this case iron,⁶ and one of two cathodic reactions. If oxygen is present, the cathodic reaction is reduction of oxygen,⁷ and in the absence of oxygen, the cathodic reaction is reduction of protons followed by formation of hydrogen gas.⁸ Equilibrium potentials calculated from free energy data,²⁴ assuming 25°C and 10^{-6} M Fe^{2+} :



This simplified model is a good approximation as long as the corrosion takes place in a simple chemical environment. In many cases, however, the environment includes a wide variety of factors that

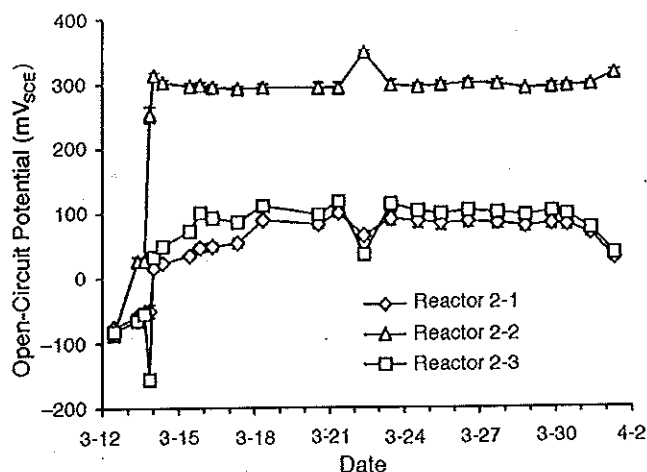
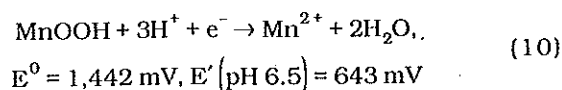
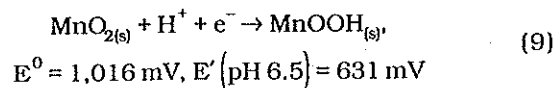


FIGURE 7. OCP of type 316L SS samples in the presence of corroding mild steel. 2-1: growth media with manganese, 2-2: growth media with manganese and bacteria, 2-3: growth media with bacteria.

can complicate the corrosion processes including microbial activity. Much effort has been committed to study and understand the processes in which microbial activity affects corrosion, but the numerous proposed mechanisms are still based upon the three reactions.²⁵⁻²⁶ Only the proposed mechanisms of corrosion influenced by sulfate-reducing bacteria have introduced other possible cathodic reactions.²⁷⁻²⁸ This and previous studies concerning the effect of biologically deposited manganese minerals on corrosion processes have discussed the possibility of a third group of cathodic reactions: reduction of manganese minerals.

Biomined manganese has been reported as being MnO_2 ,⁷⁻⁸ or a mixture of MnO_2 and MnOOH .^{4,29} It was shown earlier that the forced electrochemical reduction of MnO_2 ,⁷⁻⁸ at a rate of $2 \mu\text{A}/\text{cm}^2$ ($0.31 \mu\text{A}/\text{in.}^2$) and pH 6.5, goes through MnOOH ⁹ to Mn^{2+} ,¹⁰ [Mn^{2+}] = 10^{-6} M. It also was demonstrated that the second step takes place at a higher rate than the first, thus there is little or no accumulation of MnOOH at the surface.⁷



In natural systems, it is quite possible that oxygen, protons, and manganese oxides are present at the same time and place. Which one of the reactions will dominate is determined by the thermodynamic and kinetic properties of the system. By comparing the

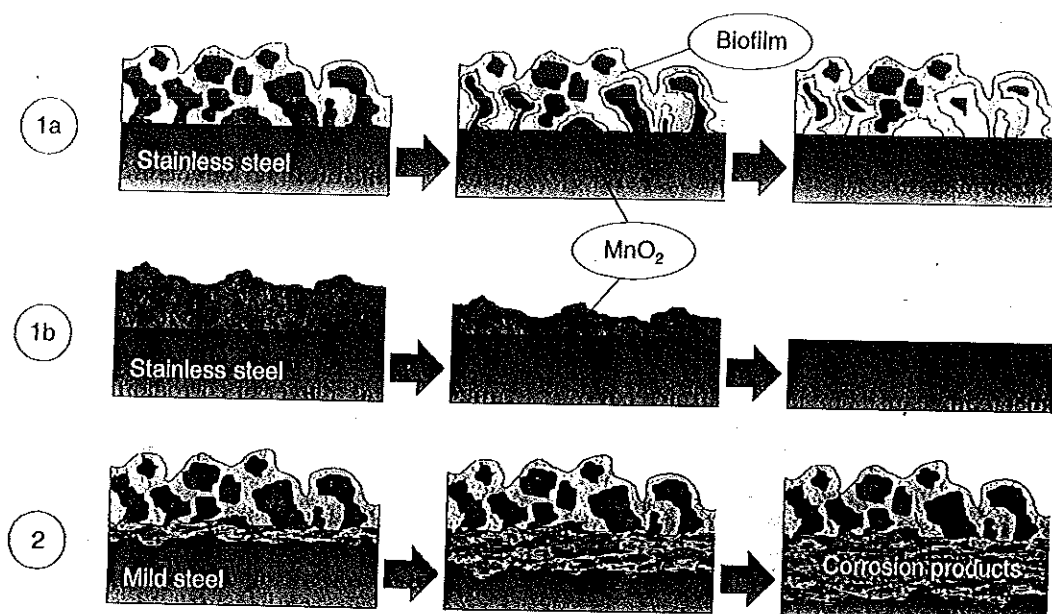


FIGURE 8. Hypothetical behavior of MnO_2 under three experimental conditions. 1(a): SS with biomineralized MnO_2 , 1(b): SS electroplated with MnO_2 , and 2: mild steel with biomineralized MnO_2 .

equilibrium potentials for the above cathodic reactions, it is clear that in an anaerobic environment, the reduction of manganese minerals will be thermodynamically favored compared to the proton reduction. The potential difference between the anodic iron dissolution and the cathodic reaction is far greater for manganese reduction than it is for proton reduction.⁶ In an aerobic environment, however, the oxygen has the highest thermodynamic potential, but since the two reactions are so close in terms of potential, kinetic effects may influence the reaction sequence.^{7,9} Oxygen reduction is known to be kinetically slow.

The present experiments with separated anode (C1008 mild steel) and cathode (type 316L SS) showed that in an aerobic environment, the galvanic current increased when the cathode was covered with MnO_2 . There are a few possible explanations for this behavior. It has been demonstrated that different manganese minerals (e.g., MnO_2 and $MnOOH$) can catalyze cathodic oxygen reduction.³⁰⁻³¹ According to these reports, the mere presence of manganese minerals should be enough to increase the rate of oxygen reduction and thus the corrosion current. In the present experiments, however, the galvanic current did not stay elevated but decreased to normal values after a while. If the effect was caused by oxygen reduction catalysis, the galvanic current should have remained elevated, but that was not the case. In the kinetic experiments, using SS cathodes electroplated with MnO_2 , the magnitude and duration of the initially elevated galvanic current increased with the amount of deposited MnO_2 . Visual observations of

the cathode showed that the manganese mineral (yellow/brownish film) disappeared from the SS cathode after it was coupled to the mild steel anode. Also, OCP of the SS cathodes had returned to preplating values. Assuming that the manganese oxide reduction took place at the water/mineral interface rather than at the metal/mineral interface, a higher surface area of the mineral deposits would result in a higher galvanic current. Figure 5 shows that the current during the first 10 s to 20 s of the experiments depended upon the amount of mineral on the surface, possibly because of different effective surface areas of the mineral deposits. After this initial phase, the current decreased and leveled off at roughly the same value for each of the three experiments. During this time, the rough samples, transferring a relatively high current, might have lost their roughness and the surface area of all samples approached the same values. After an additional period of time, depending upon the amount of mineral, the current decreased to values similar to the control experiment. The existence of such plateaus has been described previously in relation to the reduction of manganese oxides.^{1,7} As long as the plateau lasts, all reactants in the ongoing reaction are present, but sudden drops of the potential indicates that one or more reactants are depleted and the potential, thus the current, will reach values corresponding to the next possible reaction. Based on these results and the thermodynamic properties for the two reactions,^{7,9} it was concluded that the reduction of MnO_2 ⁹ is kinetically faster and more favorable than the reduction of oxygen.⁷ It is well known that oxygen reduction on metal surfaces is

relatively slow. Also, the oxygen has to diffuse from the bulk solution to react at the metal surface, whereas the manganese minerals already are present and in electrical contact with the surface.

A comparison between the two experiments with separated anode and cathode (Experiments 1[a] and [b]) showed that the same processes took place in the biological (Experiment 1[a]) and chemical (Experiment 1[b]) experiments. Figure 8 (Experiments 1[a] and [b]) illustrates hypothetical behavior of the manganese mineral in the two cases. The galvanic current was smaller in the biological experiments, which was expected because of a lesser surface coverage in this case. Electroplated samples were covered completely with the mineral film. In the biological experiments, samples were covered with a heterogeneous biofilm containing the mineral. It has been stated elsewhere that SS ennoblement by *L. discophora* includes a surface coverage of ~ 20% with manganese oxides.^{1,2} It also has been shown that the ennoblement of SS occurs when only a few percent of the surface is covered with MnO_2 .⁶ In the biological experiment, the coupling of the SS cathode and the mild steel anode did not remove all manganese minerals from the cathode surface; there still were remains of yellow/brown mineral deposits within the biofilm after the galvanic current had decreased and the experiment was terminated. Since the biomineralized manganese deposits are porous, most of the oxide probably was isolated from the metal surface at the final stage of the reduction process (Figure 8[1(a)]). It was expected that only the oxide remaining in electrical contact with the metal could be reduced.

It was concluded that if the anode and cathode are separated, biomineralized manganese deposited on the cathode can increase the galvanic current and thus the corrosion rate of a mild steel anode. The magnitude and duration of the elevated current or corrosion rate is determined by the surface coverage, porosity, and amount of deposited mineral on the cathode.

When the anode and cathode were not separated, but coexisted at the same mild steel surface, the experiment did not show any difference, whether MnO_2 was present or not. In fact, there was no significant difference in the corrosion rate of the mild steel between any of the three experimental reactors (2-1, 2-2, and 2-3). The SS control samples in Reactor 2-2 (with manganese and bacteria) ennobled similar values to previously published values.^{3,6-7} Also, there were visible brownish deposits on all surfaces inside this reactor, indicating deposition of manganese minerals. SS control samples in Reactors 2-1 and 2-3 ennobled slightly to 70 mV_{SCE} to 90 mV_{SCE}, which is quite high for SS in fresh water at neutral pH. In earlier experiments with ennoblement of type 316L SS,^{3,6-7} the reference samples did not enoble,

but their potential stayed at ~ -100 mV_{SCE}. The only difference between this and previous studies is the presence of ferric and ferrous iron resulting from the corrosion of the mild steel.^{3,6-7} Thus, it is possible that the corroding mild steel to some extent induced ennoblement through the chemical and/or microbial deposition of iron oxides onto the SS control samples in Reactors 2-1 and 2-3.

During the formation of biofilm in the reactors and the ennoblement of the SS samples, the mild steel samples were corroding. Having oxygen reduction as the cathodic reaction, the corrosion was uniform, and a layer of corrosion products in the form of iron oxides was formed long before the biological deposition of manganese started. Iron oxides generally have low electrical conductivity, and it is believed that the products from the corrosion of the mild steel acted as an electrical insulating barrier between the bulk metal and the deposited manganese mineral (Figure 8[2]). To be reduced electrochemically, the manganese minerals had to be in direct contact with the metal. In this case, the corrosion products were protecting the mild steel from the effects of biomineralized manganese.

Looking at some of the consequences of these findings, it was shown that biomineralized manganese did not influence the corrosion of mild steel alone. Thus, manganese-oxidizing bacteria can not be expected to cause elevated corrosion rates caused by the deposition of manganese oxides in systems solely built of mild steel. However, it was shown that if the manganese oxides were deposited onto a passive metal in electrical contact with the mild steel, the corrosion rate of the mild steel increased significantly. In many systems constructed of active and passive metals in electrical contact with each other, deposited manganese oxides can cause great damage to the active parts of the system. Most drinking water distribution systems, for instance, have been built in active metals like cast iron and mild steel. However, some of the crucial parts within the systems, often storage tanks, filters, etc., and often modifications to the existing distribution system have been constructed in SS. In these cases, it is highly probable that manganese minerals deposited within the SS installations will cause accelerated corrosion within the rest of the system, especially the pipelines.

CONCLUSIONS

- ❖ Biomineralized MnO_2 , deposited within biofilms of *L. discophora* on SS cathodes, increased the corrosion rate of galvanically coupled mild steel anodes about eight times, compared to a similar control experiment without manganese. The magnitude and duration of the elevated corrosion current correlated with the amount of manganese mineral deposited on the surface.

❖ The cathodic reduction of MnO_2 was significantly faster than the reduction of oxygen, even though the thermodynamic potentials of the two reactions were quite similar.

❖ Deposition of biomineralized manganese oxides on the surface of mild steel did not increase the corrosion rate, possibly because the corrosion products electrically insulated the biologically deposited minerals from the underlying metal and thus inhibited the cathodic effect of the mineral.

ACKNOWLEDGMENTS

This work was supported by the Faculty of Engineering and Science, Aalborg University, Denmark; the United States Office of Naval Research under the AASERT program, contract number N00014-92-J-1966, under ONR contract number N00014-95-1-0900; and by Cooperative Agreement EEC-8907039 between the National Science Foundation and Montana State University, Bozeman, MT.

REFERENCES

1. W.H. Dickinson, F. Caccavo Jr., Z. Lewandowski, *Corros. Sci.* 38, 8 (1996): p. 1,407-1,422.
2. W.H. Dickinson, Z. Lewandowski, *Biofouling* 10, 1-3 (1996): p. 79-93.
3. W.H. Dickinson, F. Caccavo Jr., B.H. Olesen, Z. Lewandowski, *Appl. Environ. Microbiol.* 63, 7 (1996): p. 2,502.
4. P. Linhardt, "Failure of Chromium-Nickel Steel in a Hydroelectric Power Plant by Manganese-Oxidizing Bacteria," in *Microbially Influenced Corrosion of Materials*, eds. E. Heltz, H.-C. Flemming, W. Sand (New York, NY: Springer Berlin Heidelberg, 1996): p. 221-230.
5. P. Linhardt, *Werkst. Korros.* 45 (1994): p. 79.
6. P. Linhardt, *Biodegradation* 8 (1997): p. 201.
7. B.H. Olesen, R. Avci, Z. Lewandowski, *Corros. Sci.* (1999).
8. B.H. Olesen, R. Avci, Z. Lewandowski, "Ennoblement of Stainless Steel Studied by X-Ray Photoelectron Spectroscopy," *CORROSION/98*, paper no. 275 (Houston, TX: NACE, 1998).
9. S.C. Dexter, J.P. LaFontaine, *Corrosion* 54, 11 (1998): p. 851.
10. M.H.W. Renner, G.H. Wagner, *Stainless Steel World* 11 (1996): p. 36-43.
11. B. Little, P. Wagner, F. Mansfeld, *Int. Mat. Rev.* 36, 6 (1991): p. 253.
12. M.H.W. Renner, *Dechema Monogr.* 133, 59 (1996), p. 59-70.
13. M.J. Franklin, D.E. Nivens, J.B. Guckert, D.C. White, *Corrosion* 47 (1991): p. 519.
14. D. Emerson, W.C. Ghiorse, *Isolation, Appl. Environ. Microbiol.* 58, 12 (1992): p. 4,001-4,010.
15. R.L. Gherna, P. Gerhardt, eds. *Preservation, Manual of Methods for General Microbiology* (Washington, DC: American Society for Microbiology, 1981).
16. B.J. Webster, R.C. Newman, *Corros. Sci.* 35, 4 (1993): p. 675.
17. G. Chen, R.J. Palmer, D.C. White, *Biodegradation* 8 (1997): p. 189.
18. M. Urquidí-Macdonald, S. Real, D.D. Macdonald, J. *Electrochem. Soc.* 133, 10 (1986): p. 2,018.
19. H. Shih, F. Mansfeld, *Corros. Sci.* 28, 9 (1988): p. 933.
20. *Zplot for Windows — Electrochemical Impedance Software Operation Manual* (South Pines, NC: Scribner Associates, Inc., 1997).
21. R.L. Hurt, J.R. Macdonald, *Solid State Ion.* 20 (1986): p. 111.
22. J.R. Macdonald, *Solid State Ion.* 15 (1985): p. 159.
23. A.J. Bard, L.R. Faulkner, *Electrochemical Methods — Fundamentals and Applications* (New York, NY: John Wiley and Sons, 1980).
24. A.J. Bard, R. Parson, J. Jordan, *Standard Potentials in Aquatic Solutions* (New York, NY: Marcel Dekker, Inc., 1985).
25. E. Heltz, H.-C. Flemming, W. Sand, eds., *Microbially Influenced Corrosion of Materials* (New York, NY: Springer Berlin Heidelberg, 1996), p. 5-143.
26. W.P. Iverson, *Adv. Appl. Microbiol.* 32 (1987): p. 1.
27. R.S. Dubey, T.K.G. Nambodhri, S.N. Upadhyay, *Indian J. Chem. Technol.* 2 (1995): p. 327.
28. W. Lee, Z. Lewandowski, P.H. Nielsen, W.A. Hamilton, *Biofouling* 8 (1995): p. 165.
29. L.F. Adams, W.C. Ghiorse, *Geochim. Cosmochim. Acta* 52 (1988): p. 2,073.
30. H.S. Horowitz, J.M. Longo, *Mat. Res. Bull.* 13 (1973): p. 1,359.
31. K. Matsuki, H. Kamada, *Electrochim. Acta* 31, 1 (1986): p. 13.

NACE INTERNATIONAL OFFERS RESEARCH SEED GRANT FUNDING

NACE International's Research Committee is soliciting proposals for one \$20,000 research seed grant. The grant period will be from July 1, 2000 through June 30, 2001, and could be extended for one additional year.

The grant is funded by the U.S. Office of Naval Research and supported by NACE.

The grant is intended to encourage new researchers to study the corrosion of engineering materials.

Grant recipients will be selected at CORROSION/2000,

scheduled for March 26-31, 2000, in Orlando, FL.

Proposals should include:

- a description of the proposed research project, including goals and specific objectives (not more than three double-spaced pages);

- a description of how the grant might be used to obtain additional support from other organizations;

- background on the principal investigator;

- a proposed budget (funds may not be used to support univer-

sity indirect costs/overhead); and — a description of other programs underway that might strengthen the proposal.

Appendices may be attached, but brevity is encouraged.

The original and five copies of the proposal should be sent no later than February 1, 2000, to: Chris Kilmer, Director, Technical Activities Division, NACE International, Research Committee Seed Grant Program, PO Box 218340, Houston, TX 77218-8340 (shipping address: 1440 South Creek Drive, Houston, TX 77084-4906).